Pinhole Camera Sun Finders: On Field Characterization

Gianluca Marotta[1], Daniela Fontani[1], Franco Francini[1], David Jafrancesco[1] and Paola Sansoni[1]

[1] CNR-INO Istituto Nazionale di Ottica, Largo E. Fermi, 6 – Firenze - 50125 – Italy

Phone: +39-055-23081; e-mail: daniela.fontani@cnr.it

Abstract

The use of sun finders is essential to optimize the performance of solar concentration systems. A sun finder based on the pin-hole camera principle has been developed for Concentrating Photo Voltaic systems, which require pointing precision of the order of 0.01 angular degrees. Several configurations of this device were implemented and they were tested in laboratory and outdoor. This paper discusses the outdoor characterization of a set of sun finders, analyzing the results. Features and performances measured in real conditions are in good agreement with the data obtained in the laboratory, under controlled and reproducible conditions. The field of view of the sun finder can be customized by varying the pinhole-detector distance allowing to use it in many applications. Even if the results show that the pointing precision exceeds 0.01 degrees, the sun finder is simple, useful, adjustable and economic.

Keywords: sun tracking; sun finder; optical sensor; solar energy; optical test; solar concentration.

1. Introduction

Sun tracking is a key feature for each technology that uses optical systems for sunlight concentration (Lee et al. 2009; Mousazadeh, H et al. 2009). Systems operating in the CSP (Concentrating Solar Power) or CPV (Concentrating Photo-Voltaic) sectors need to be accurately aligned with the solar rays in order to focus them on the active region of the receiver. Any error on the sun tracking would affect the intercept factor of the system, namely the ratio between the sun rays that reach the receiver and those that cross the aperture. The intercept factor is one of the terms that contribute to the optical efficiency of the concentrator, so a better-performing sun tracking could improve the global efficiency of the solar energy exploitation system.

Two methods are currently in use for this purpose: the first one (passive tracking) is based on the "ephemeris tables". They contain astronomical calculations that can predict the position of the sun in a specific location of the Earth for each moment of the year (Chen et al. 2006). The second method (active tracking) utilizes a dedicated device, namely the "sun finder", which directly measures the position of the sun. In this case, the sun finder gives a continuous feedback to the tracking system, allowing to bypass the systematic errors typical of the ephemeris-based tracking control. Indeed, for the passive tracking systems, it can be difficult to keep a high mechanical stability; for example because of the wind action, or due to little mechanical jams of the tracking motors. In fact, systems based on ephemerides need to be calibrated often, in order to reduce this kind of errors (Parmar et al. 2015).

For linear concentrators, like parabolic troughs, a simplified guiding system rotates the solar trough only in one direction. Two configurations are possible in this case: the linear axis of the mirror can be placed along the Nord-South direction, while the tracking follows the daily sun motion from East to West, or the mirror axis can be located along the East-West direction, while the tracking is performed to reach the correct sun altitude that varies seasonally (Sansoni et al. 2015). In both cases the opto-electronic device for tracking utilizes couples of photo-detectors that, in conditions of alignment in the solar rays' direction, supply the same response because they detect the same amount of light (Huang et al. 2009). The simplest device is composed of an opaque sector, which separates two photodiodes (Salawu and Oduyemi 1986). In alternative, similar optical configurations can be used to project shadows on the detectors: for instance two crossed opaque sectors or a rod centered on a screen (Rouan et al. 2000).

Concentrating PhotoVoltaic (CPV) plants and Solar Dishes CPV systems can work only with direct sunlight, so

doi:10.18086/swc.2019.02.01 Available at http://proceedings.ises.org

they need to use an active pointing system. In this case an enhanced pointing accuracy can be obtained employing an optical system with a focal length F, such as a lens, which projects the sun's image on photo-detectors. Since the sun has abundant luminous intensity, the lens can be replaced with a tiny pinhole, creating a so-called "pin-hole camera" (Fontani et al. 2007). This kind of device projects the sun's image in the same way as a lens could do, but with a much cheaper realization.

Sun finders equipped with an optical system are also utilized as astronomical pointing devices. Recently techniques based on image processing have also been applied to solar tracking (Fontani et al. 2011).

In this paper we propose a characterization of Pinhole Camera Sun Finders (sun finders). The study is made in operative conditions, namely with the sun finder mounted on a sun tracker exposed to solar radiation**.**

2. Pinhole Camera Sun Finders

The sun finders studied in this paper are very simple and cheap to realize. They are based on the principle of the pin-hole camera. Sun rays enter through the pin-hole aperture and reach a 4Q (four quadrants) detector, whose surface is perpendicular to the optical axis of the device (in red in Fig. 1(a)). This kind of detector is composed of four independent squared photodiodes placed on the same surface. Each photodiode generates a photo-current that is proportional to the light that arrives on it. The distance between pin-hole and 4Q detector (L) is the parameter that characterizes the different sun finders studied. The field of view can be customized by varying the pinhole-detector distance allowing to use it in many applications.

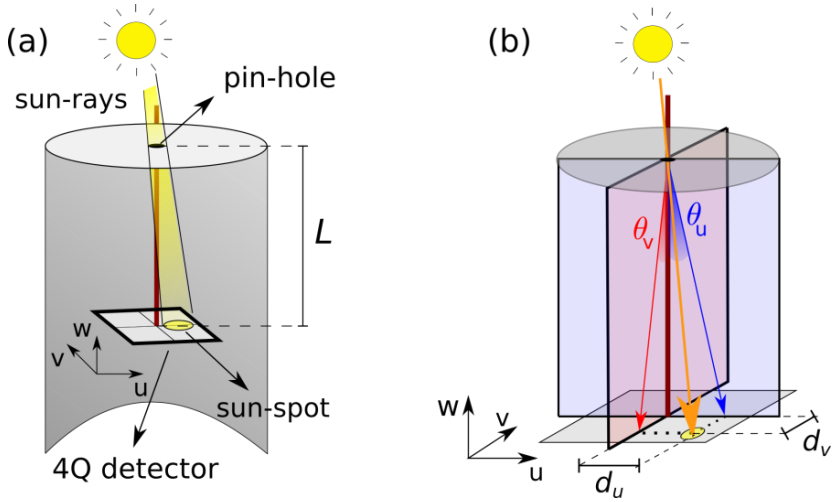

Fig. 1 (a) Sketch of the Pinhole Camera Sun Finder. Sun rays enter through the pinhole and intercept the 4Q detector which is perpendicular to the optical axis (red line). (b) Principle of measure of the sun position. Orange arrow represents the sunray that passes through the center of the pinhole aperture, while blue line and red line represent the projections of the sun-ray onto the u-w plane and the v-w plane, respectively.

The sun can be considered as a light source located at an infinite distance, so the solar rays are considered almost parallel. Anyway, the position of the sun with respect to a surface can be expressed by two angles. In the reference system of the Earth surface, the two angles in use are the "elevation angle", namely the complementary of the angle that the sun rays form with the zenith direction, and the "azimuth angle", the angle that the projection of the sun rays on the Earth surface forms with the Nord-South direction (Bhatia 2014).

In the reference system of the detector, indicated by the *(u,v,w)* axes in Fig. 1, it is useful to define a new couple of angles to describe the sun position. In this case the two angles θ_u and θ_v, indicated in Fig. 1(b), are in use. They are, respectively, the angle between the optical axis and the projection of sun rays onto the *u-w* plane (θ_u) and the *v-w* plane (θ_v,). As the figure shows, the coordinates of sun-spot center, with respect to the detector's center, d_u and d_v in Fig. 1(b), are directly proportional to the sinus of angles θ_u and θ_v.

Unfortunately, a detector like the 4Q–detector has the advantage of having a cheap cost, but is not able to measure these coordinates for each sunspot position. In fact, the only possible data that it gives are the four voltages, each of which is proportional to the photocurrent generated on each quadrant. With reference to Fig. 2(a), indicating

the voltages with V_i (i=1,2,3,4) referred to quadrants Q_i, we can define the new parameters

$$P_u = \frac{(V_1+V_2)-(V_3+V_4)}{V_1+V_2+V_3+V_4} \qquad (1)$$

$$P_v = \frac{(V_1+V_4)-(V_2+V_3)}{V_1+V_2+V_3+V_4} \qquad (2)$$

The meaning of these two variables can be understood in the following way: they give a measure of relative alignment of the 4Q-detector with respect to the direction of solar rays. When the area of sun-spot is completely in one quadrant the values of (P_u,P_v) will be ± 1 with four combinations that individuate the four quadrants. With reference to Fig. 2(a), if the spot area reaches only Q_4, V_4 is the unique non-zero voltage signal , so $P_u = -1$ and $P_v = +1$. Otherwise, if the center of the spot lies in the green region of Fig. 2(a), it means that the spot area lies at least in one another quadrant and the values of P_u and P_v would be between +1 and -1. Furthermore, when the spot center is perfectly in the center of the 4 quadrants, namely the sun ray is aligned with the optical axis of the sun finder, $(P_u, P_v) = (0,0)$.

A typical behavior of the parameter P_u (P_v) is shown in Fig. 2(b).

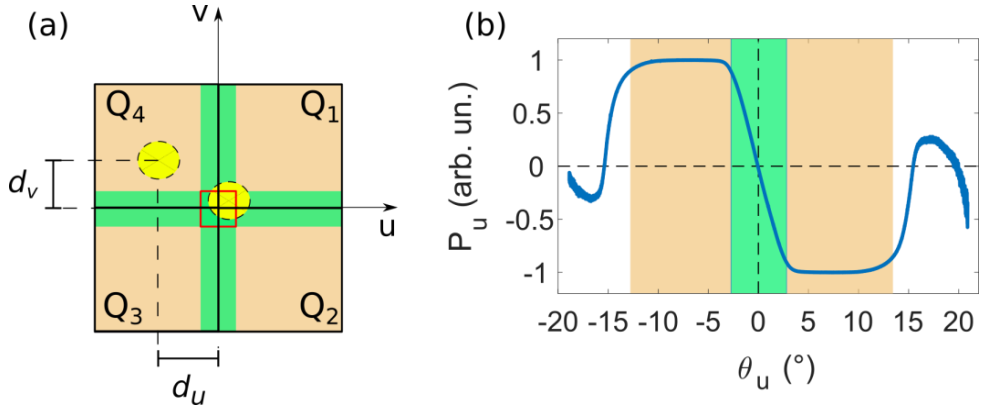

Fig. 2 (a) Sketch of the different regions in the 4Q – detector. (b) Measure of P_u for a Pinhole Camera Sun Finder with L = 6.6 mm. The green zone indicates the "monotone region" where P_u (P_v) corresponds to a unique value of θ_u (θ_v), while the FOV of the sensor is indicated with the light orange background.

The green region of Fig. 2 is identified as “monotone region”, because in this region there is a unique correspondence between P_u (P_v) and θ_u (θ_v), almost linear, so the measure of the four voltage signals gives at least one of the two angles of the sun position in an unambiguous way. When the spot lies in the red rectangle of Fig. 2(a), both angles could be measured.

When the sunspot falls outside the 4 quadrants all voltage values go to 0 and P_u (P_v) is only affected by the noise of the electronic device. This region is identified as “out of the FOV” of the sensor, indicated with a white background in Fig. 2(b); where FOV is the Field Of View of the sensor, which corresponds to the light orange background. In this region is possible to determine only the direction of the sun position with respect to the detector center.

3. Experimental setup

The purpose of the present study is to characterize several Pinhole Camera Sun Finders in operative conditions, namely when they are under the solar radiation. For this purpose, the sun finders are mounted on a sun tracker, shown in Fig. 3(a).

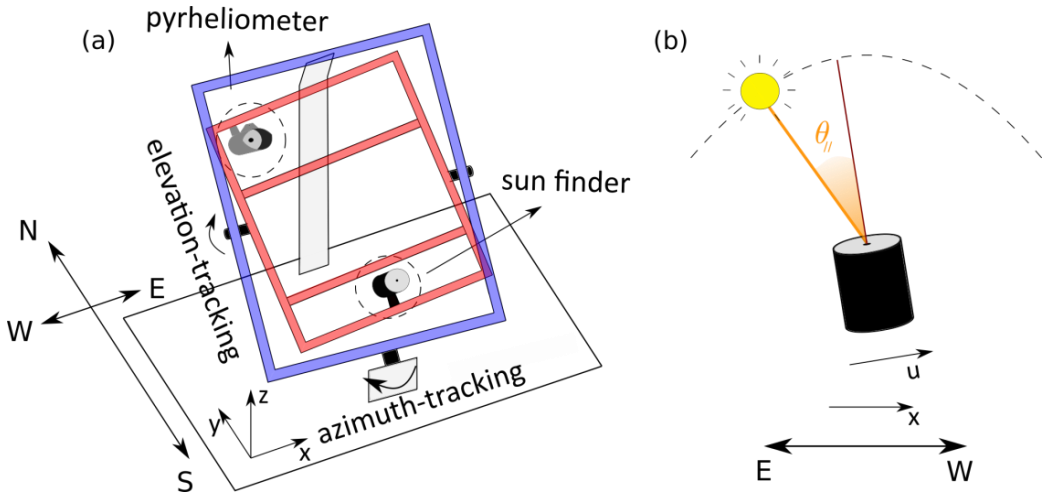

Fig. 3 (a) Sketch of the sun tracker utilized for the sun finder characterization. The internal frame is for elevation-tracking and is colored in red while the external one is for azimuth-tracking and colored in blue. (b) Sketch of the experiment. While the tracker follows the sun along the elevation angle, the sun proceeds in its daily path (dotted line), allowing a measure of θ_u.

The Sun Tracker is composed of two frames that can rotate separately in order to follow the sun along its daily motion. The external frame follows the variation of the azimuth angle ("azimuth-tracking"), while the internal one follows the variation of the elevation angle ("elevation-tracking").

The rotation axis of the azimuth-tracking is placed so that its projection on the Earth's surface (xy plane in Fig. 3(a)) is coincident with the North-South direction. The same axis is inclined with respect to the Earth's surface of an angle of 43.8°, same of the latitude of Florence. The rotation axis of the elevation-tracking is fixed on the external frame and parallel to the azimuth-tracking axis. It is worth to note that this alignment is just a positioning of convenience: with this configuration, the movements of the tracker are reduced to a minimum. Nevertheless, it does not mean that the tracker is not able to follow the sun in many other configurations.

A pyrheliometer is also mounted on the sun tracker. It is used both as an alignment reference and for collecting the data of the DNI (Direct Normal Irradiance) during the experiment.

4. Alignment and Measurement procedures

In order to execute the measurements the following steps are performed.

First of all, the tracker is positioned so that the sunrays are perpendicular to the plane of the internal frame. For this purpose, a tiny hole placed on the pyrheliometer is utilized: it projects a sunspot on a second hole placed at a distance of about 20 cm. When the spot passes through both holes, the sun is considered aligned with the direction perpendicular to the frame plane.

When this alignment is reached, the sun finder is tilted by means of a specific movement with two screws to have P_u and P_v equal to zero. This corresponds to the situation in which the detector plane is parallel to the plane of the internal frame of the sun tracker.

After that, the sun finder is rotated around the *w*-direction, in order to align the *u* direction (or *v*) of the 4Q-detector with the x-axis, which represents the East-West direction (Fig. 3(b)). To do this it is necessary to check the values of P_u (or P_v) while the tracker executes its azimuth-tracking and elevation-tracking movements. For example, to align the *u*-direction of the sun finder with the direction East-West of the Earth, it is necessary to assure that a movement of the elevation-tracking does not affect the P_u value, that has to remain zero. Similarly a movement of the azimuth-tracking has to keep $P_v = 0$. The same procedure has to be followed to align the *v*-direction, where P_u and P_v are exchanged.

As in the previous laboratory measurements (Fontani et al. 2018), the sun finders are characterized for both *u* and *v* directions, separately. The examined direction (*u* or *v*) will be the one aligned with the x-direction, with the procedure explained above. In the following, P will indicate the variable under examination (P_u or P_v) and so θ (θ_u or θ_v) the respective angle. All the measurements are made with the elevation-tracking enabled, this allows

that only the variable under examination varies. To complete the elevation-tracking, the same sun finder is in use as a feedback sensor.

To achieve the measurement the azimuth-tracking is initially moved so that θ goes out of the FOV of the sun finder, with the sun positioned at East with respect to the optical axis (Fig. 3(b)). Then the sun proceeds in its daily motion, going toward West, it passes through the position aligned with the optical axis of the sun finder (θ=0) and then goes again out of the FOV on the other side of the pointer. In this way it is possible to afford a complete angular study of the sensor.

A suitable acquisition system allows to save the values of the four voltage signals (V_i) as the time (t) varies. After that, P is calculated with the formulas (1) or (2). To define an uncertainty for V_i, the electrical noise (N_i) is recorded acquiring V_i with the entrance pinhole closed, in order to ensure that no light goes inside the sun finder. The mean value of N_i is kept as an offset to be subtracted to V_i, while its standard deviation is used as the uncertainty of the voltage signals (δV_i). The uncertainty of P is calculated propagating the error on its formula.

The time measurement is converted into an angular value and since the time resolution of the acquisition system is $\sim 0.01\ s$, the angular resolution will be about 10^{-5} °.

In its motion, the sun goes also into the FOV of the pyrheliometer, allowing a measure of the DNI during the duration of the experiment. These data measure the environmental conditions, in which the outdoor characterization of the sun finders was performed.

5. Study of the sensitivity

The sensitivity of the sensor is defined as the smallest variation of θ that the device can associate to a variation of P. With this definition, it represents the accuracy with which the sun finder is able to determine the sun position. Obviously, it makes sense to define it only in the monotone region of the sensor.

As Fig. 4 shows, the behavior of the data in an angular range close to the resolution of the acquiring system is not so regular. It can be seen a presence of casual errors in the behavior of P, these errors increase the uncertainty previously defined. These casual errors are due probably to small movements of the tracker. This means that the study of the sensitivity will give different values depending on the region of θ considered.

The following procedure is performed to avoid this difficulty and to measure a reliable quantity. For each data a "punctual sensitivity" (k) is defined. It is the minimum interval for θ for which all the consequent P values have their superior limit of uncertainty lower than the inferior limit of the uncertainty of the data of interest.
Following the example of Fig. 4, the "punctual sensitivity" k of the red-colored data is highlighted in green, and it is possible to see that all the data after this interval are below the inferior limit of its uncertainty, represented by the dashed line.

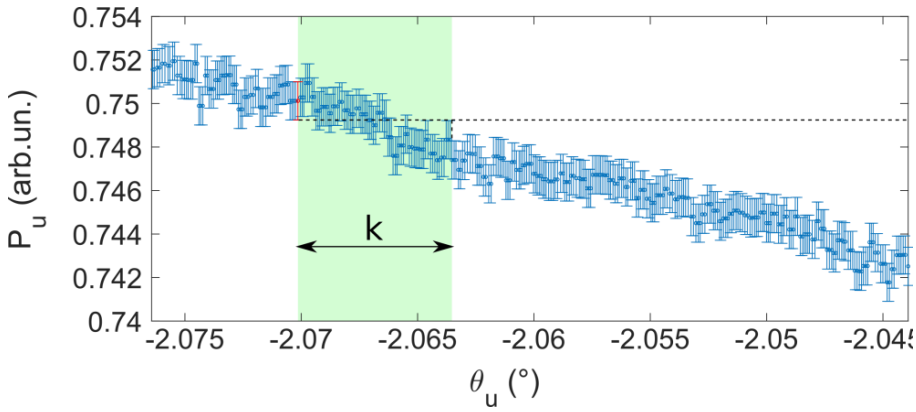

Fig. 4 Example for the study of the sensitivity. The plot shows a small portion of the characterization in the *u*-direction for the sun finder with L = 6.6 mm. The green region highlights the k value for the point colored in red. The dashed line is in correspondence of the inferior limit of the uncertainty range of this value.

Figure 5 shows an example of the behavior of the "punctual sensitivity" k when θ varies. The sensitivity can be defined as the mean value of this distribution, represented by the dashed line in Fig. 5. It is important to remind that these measurements are made in the "monotone region".

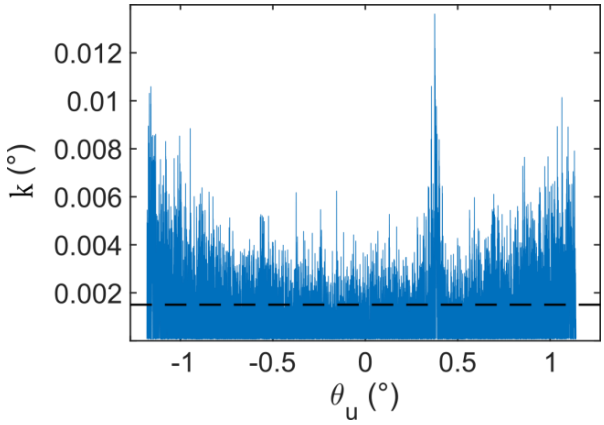

Fig. 5 Distribution of the punctual sensitivity k as a function of θ. The dashed line indicates the mean value. Data refer to the sun finder with L = 19.5 mm.

6. Studies of FOV region and monotone region

Referring to Fig. 2(b), in Sect. 2 the monotone region (in green in Fig. 2(b)) has been defined as the central portion of the curve, where P decreases monotonically with respect to θ. P is the variable under examination (P_u or P_v) and θ (θ_u or θ_v) the respective angle. Concerning the FOV (Field Of View), which is the whole angular aperture of the sensor. In Fig. 2(b) is indicated with the light orange background and represents the zone where the sun is detected by the sensor also if it is not possible to determine exactly the position but only the direction where the sun is located with respect to the device axis. The white zone in Fig. 2(b) has been called the "region out of the FOV" of the sensor, where the sun position is missed.

As in the previous laboratory study (Fontani et al. 2018), the limits of FOV are defined as the angle for which the module of P reaches the value of 90% of the max before it collapses in the noisy "region out of the FOV". As the same, the limits of the "monotone region" are the values of θ for which the module of P reaches 0.9, before it becomes 1.

However it is impossible to determine without ambiguity these angular limits, because of the uncertainty and the casual error shown in Fig. 4. It can be observed that the casual oscillation affects the forth decimal of P, so the data can be rounded to the thousandth without significant loss of information. After that, the limits of the region of interest (monotone or FOV) are defined as the median of the angles that correspond to a value of the module of 0.900. The range of the set of angles defines the uncertainty of the limits values calculated.

7. Summary of results.

The results of the outdoor experimentation of three different Pinhole Camera Sun Finders are presented in Fig. 6 and Table 1. The sun finders are identified by the distance between pin-hole and 4Q-detector L (see Fig. 1).

As it could be easily understood, an increasing distance between pin-hole and 4Q-detector L corresponds to a minor extension of the monotone region and to a smaller FOV. This behavior is well described in Fig. 6 that shows the variation of P_u as a function of the angle θ_u for the three sun finders under examination.

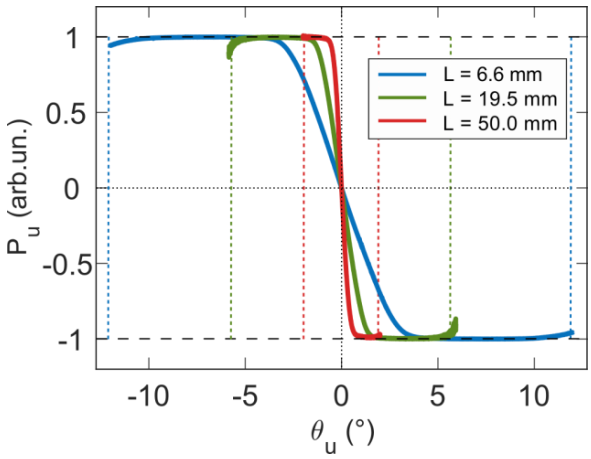

Fig. 6. Experimental data of P_u as a function of θ_u for the three sun finders under examination. Each couple of colored dashed lines indicates the FOV of the corresponding sensor.

The experimental results are synthetized in Table 1, where the values both for *u*-direction and *v*-direction are reported. It is possible to see that the values are almost the same in both directions, except for small differences, possibly due to little errors in the alignment procedures.
The mean DNI is also reported with its standard deviation, with the operation of mean implemented for all the values recorded in the FOV of the pyrheliometer. It can be inferred that the sun finders can operate under the same conditions in a DNI range between around 700 W/m^2 and 900 W/m^2.

Table 1: Summary of the characteristics of the sun finders examined outdoor for both directions

	Pinhole-detector distance - L (mm)	**Direction**	**Sensitivity (mean)**	**Sensitivity (max)**	**Width of the "Monotone region"**	**Field Of View**	**DNI (W/m^2)**
sun finder 1	6.6	*u*	0.003°	0.03°	(5.5 ± 0.1) °	(25.0 ± 0.1)°	861 ± 4
		v	0.003°	0.03°	(5.9 ± 0.2) °	(25.0 ± 1.2)°	901 ± 4
sun finder 2	19.5	*u*	0.002°	0.014°	(2.36 ± 0.02) °	(11.79 ± 0.17) °	824 ± 5
		v	0.001°	0.011°	(2.31 ± 0.02) °	(11.83 ± 0.19) °	784 ± 3
sun finder 3	50	*u*	0.002°	0.015°	(1.019 ± 0.006) °	(5.38 ± 0.74) °	744 ± 5
		v	0.002°	0.013°	(0.828 ±0.008) °	(4.92±0.26)°	702 ± 4

A previous study (Fontani el al. 2018), was directed to characterize the same devices in the laboratory. In this case, the sun rays were replaced by a laser beam passing through a beam expander, so with no divergence, and the movement of the sun was simulated with a mechanical rotator that mounted the sun finder under examination. The laboratory measurements aimed to provide an optical characterization of the devices in replicable conditions, determining the angular range of the "monotone region", the angular sensitivity and the FOV of the device.

Table 2 reports a summary of the experimental results, comparing the laboratory measurements with the outdoor measurements. Here a mean value of the two directions (*u* and *v)* is considered. For the outdoor sensitivity, the mean value is considered.

Table 2: Summary of the characteristics of the sun finders examined in laboratory and under the sun.

		Pinhole-detector distance - L (mm)	Width of the "Monotone region"	Sensitivity	Field Of View
sun finder 1	Lab	6.6	(6.5 ± 0.2) °	0.003 °	(24.0 ± 0.2) °
	Out		(5.7 ± 0.1) °	0.003 °	(25.0 ± 0.6) °
sun finder 2	Lab	19.5	(2.6 ± 0.2) °	0.001°	(10.6 ± 0.2) °
	Out		(2.34 ± 0.02) °	0.002 °	(11.8 ± 0.2) °
sun finder 3	Lab	50.0	(1.1 ± 0.2) °	0.001 °	(4.4 ± 0.2) °
	Out		(0.923 ± 0.007) °	0.002 °	(5.2 ± 0.5) °

Outdoor measurements confirm the values obtained with laboratory tests. Moreover, the mean of the sensitivity is of the same order of magnitude (10^{-3} °). However, in the laboratory measurements, the uncertainty was obtained calculating the mean on the data of each measurement, before rotating the mechanism mounting the sun finder, in order to eliminate some effects due to noise. In the outdoor case, that represents the operative condition for the device, this kind of measurement in "stable" condition was not possible, because of the motion of the sun and of the casual error occurrence described before. Furthermore, laboratory tests were performed on a stable configuration, free of vibrations, in a way that the outdoor configuration cannot be. Nevertheless the values obtained are in agreement, thus validating the characterization made in the laboratory, which for the reasons mentioned above is more controlled and repeatable. A significant result is that the sensitivity values are in good agreement and it is particularly important that they are extremely lower than the required precision for this type of devices (Fontani el al. 2011).

8. CONCLUSIONS

The sun finder represents the core of the solar tracking device, which is necessary for systems based on sunlight concentration. When the collector is correctly aligned in the sun direction, the focused radiation is maximized and consequently the collection efficiency of the system reaches its maximum. The presented sun finder is based on the pin-hole camera principle: it couples a pinhole with a 4quadrant-detector using the displacement of the spot projected on the detector to calculate the angular displacement of the sun. Several configurations of this sensor have been practically realized and experimented in laboratory and outdoor. The results of the laboratory characterization have been presented at the SolarPACES conference 2018 (Fontani el al. 2018).

The results of the outdoor experimentation, with direct exposure to the sun, are discussed in this paper. They have been successfully compared with the laboratory results.

The different versions of sun finder are identified by the L value, which is the distance between 4Q-detector and pin-hole (in Fig. 1(a)). Geometrical features and optical parameters have been measured in different conditions in the outdoor tests with respect to the laboratory measurements. Nevertheless they are in good agreement, as the summarizing Table 2 shows.

An exemplificative result is the characterization of a sun finder (in Fig. 2(b)), which is obtained plotting the parameter P_u versus the angular displacement of the sun (θ_u). In this type of plots, two regions can be identified: the "monotone region" (in green in Fig. 2(b)) and the "FOV region" (in orange in Fig. 2(b)). The "monotone region" represents a key feature of each examined sun finder. In this region the parameter P_u varies almost linearly with the angle θ_u. Outside this region there is the so-called "FOV region", where it is possible to obtain information only on the direction of the solar movement. In fact, here the sun finder is still able to detect the sun presence, but it is not possible to have a precise measure of the sun's position.

The outdoor experimentation has confirmed the results obtained in the laboratory characterization of the sun finders. A significant result is that the sensitivity values are in good agreement and it is particularly important that they are extremely lower than the required precision for this type of devices.

9. References

Bhatia, S.C. 2014 Advanced Renewable Energy Systems, Woodhead Publishing India, Pages 32-67, ISBN 9781782422693

Chen, Y. T., Lim, B. H., & Lim, C. S. (2006). General sun tracking formula for heliostats with arbitrarily oriented axes. Journal of Solar Energy Engineering. 128(2), 245-250.

Fontani, D., Sansoni, P., Francini, F., Mercatelli, L., Jafrancesco, D., 2007. A pinhole camera to track the sun position. Proc. ISES Solar World Congress 2007, Beijing - China, 18-21 Sept. 2007, t5.1.O12.

Fontani, D., Sansoni, P., Francini, F., Jafrancesco, D., Mercatelli, L., Sani, E., 2011. Pointing sensors and sun tracking techniques. International Journal of Photoenergy. 2011, 806518, 1-9.

Fontani, D., Marotta, G., Francini, F., Jafrancesco, D., Sansoni, P., 2018. Sun finders based on a pinhole camera. Proc. SolarPaces 2018 - Casablanca 2-5 Oct. 2018.

Huang, Y. J., Wu, B. C., Chen, C. Y., Chang, C. H., & Kuo, T. C., 2009. Solar tracking fuzzy control system design using FPGA. In Proceedings of the World Congress on Engineering, 1, 1-3.

Lee, C.-Y., Chou, P.-C., Chiang, C.-M., Lin, C.-F., 2009. Sun Tracking Systems: A Review. Sensors. 2009, 9, 3875-3890.

Mousazadeh, H., Keyhani, A., Javadi, A., Mobli, H., Abrinia, K., Sharifi, A., 2009. A review of principle and sun-tracking methods for maximizing solar systems output. Renewable and Sustainable Energy Reviews. 13, 1800-1818.

Parmar, N. J., Parmar, A. N., Gautam, V. S., 2015. Passive solar tracking system. Int. J. Emerg. Technol. Adv. Eng. 5 (1), 138–145.

Rouan, D., Riaud, P., Boccaletti, A., Clénet, Y., Labeyrie, A., 2000. The Four-Quadrant Phase-Mask Coronagraph. I. Principle. Publications of the Astronomical Society of the Pacific. 112 (777), 1479-1486.

Salawu R. I., Oduyemi T. A., 1986. An electronic sun finder and solar tracking system. Solar & Wind Technology. 3 (3), 215-218.

Sansoni, P., Fontani, D., Francini, F., Giannuzzi, A., Sani, E., Mercatelli, L. and Jafrancesco, D., 2011. Optical collection efficiency and orientation of a solar trough medium-power plant installed in Italy. Renewable Energy. 36 (9), 2341-2347.

Sansoni, P., Fontani, D., Francini, F., Jafrancesco, D., 2015. Optical Sensors for Solar Pointing. Proc. ISES Solar World Congress 2015 – Daegu, Korea 8-12 Nov 2015.